ELSEVIER

Journal of Power Sources 78 (1999) 204–213

JOURNAL OF POWER SOURCES

Study of the softening of the positive active-mass in valve-regulated lead-acid batteries for electric-vehicle applications

P. Lailler [a], F. Zaninotto [b], S. Nivet [a], L. Torcheux [a,*], J.-F. Sarrau [a], J.-P. Vaurijoux [a], D. Devilliers [b]

[a] *CEAC EXIDE Europe, 5-7 allée des Pierres Mayettes, 92636 Gennevilliers Cedex, France*
[b] *Université Pierre et Marie Curie, 4 Place Jussieu, 75252 Paris Cedex 05, France*

Received 3 September 1998; accepted 27 November 1998

Abstract

Valve-regulated lead-acid (VRLA) batteries have been proposed as energy sources for electric vehicles because of their good power performance and low price. Unfortunately, however, intensive utilization of the positive active-mass causes softening of this material and, thereby, reduces battery cycle-life. Experimental cells have been developed and used in order to understand the mechanism of softening. The evolution kinetics of the β-PbO_2 has been studied with very dynamic discharge profiles: different steps of the β-PbO_2 life have been explored. The experimental results have been compared and correlated with positive active-material used in electric vehicles (field tests). Scanning electron microscopy reveals a continuous growth of the β-PbO_2 microstructure throughout the cycle-life of the active mass (from ~1 to ~2 μm). This is confirmed by a decrease in the specific surface area (from 4 to 2.5 m^2 g^{-1}). Powder X-ray diffraction reveals similar changes in the nanostructure (from ~20 to 90 nm): the crystallites, as microstructure particles, grow with the number of cycles. These results also show the difference between the active material bound to the electrode and the β-PbO_2 crystallites which have lost contact with the plate; the latter are larger than the former (~100 nm vs. ~80 nm). The investigations confirm that the capacity loss of VRLA batteries is strongly linked to a micro- and nano-textural evolution of the β-PbO_2. This finding supports the theory that there is a progressive expansion of the positive active-material, which leads to a decrease in the contact zones until final shedding of the material takes place. Strategies to overcome this effect have been tested and it appears that electrolyte additives and electrical treatments could be useful in extending battery cycle-life.

Keywords: Active material; Cycle-life; Lead-acid battery; Plate expansion; Softening; Valve-regulated

1. Introduction

Lead-acid batteries have a very large range of applications. Each use requires a specific technology in order to withstand the accompanying stress placed on the battery. Low cost, easy recycling and ready availability of raw materials are the main qualities of this battery system.

Electric vehicle (EV) applications place great demands on the battery: acceleration, braking and repetitive rests cause discharge or charge current pulses. This dynamic way of cycling tends to reduce battery life by accelerated softening of the active material of the positive plate. The sensitivity to intensive use is the principal difficulty in adapting lead-acid technology to meet the requirements of EV service.

Many studies have been devoted to characterizing changes in the active material throughout battery life. Different theories have been elaborated; some of these are based on a structural point of view, others place a greater emphasis on a textural approach. Some authors have explored the structural evolution of the active material. For example, there have been several studies [1–5] of the evolution of the α-PbO_2:β-PbO_2 ratio. The influence of this ratio on the ageing of the positive active-mass is doubtful, however, because the value of the ratio is stabilized well before failure of the battery. Boher [6] has attempted to link softening with the distribution of protons in the active mass, but such a phenomenon is quite difficult to quantify.

Studies of the nano-textural evolution seem to be a more useful way to explore changes in the active mass. Boher [6] and Hill and Madsen [7] have observed narrow-

* Corresponding author.

0378-7753/99/$ - see front matter
PII: S0378-7753(99)00038-5

ing of the full width at half maximum in the X-ray diffraction spectra of PbO_2 during cycling. They attribute this phenomenon to growth in the crystallite size of the active material connected to the electrode. Micro-textural evolution has also been observed: it has been shown [8,9] that the PbO_2 grain size grows during battery life. According to these authors, this textural evolution is linked to ageing of the positive material. The aim of this study is to understand and quantify the mechanisms of capacity loss in valve-regulated lead-acid (VRLA) batteries operating in EV applications. For this purpose, low-current discharge profiles or dynamic discharge profiles have been used. The active material has been systematically analyzed, even when disconnected from the electrode. Technical strategies have been applied in order to delay capacity loss.

2. Experimental

2.1. Electrochemical cells

VRLA cells of the absorptive glass-mat (AGM) design have been built with specifications as close as possible to those of industrial batteries. The quantity of each constituent determines the principal characteristics of the cell. For example, the amount of sulfuric acid per gram of positive active-material before formation has to be 0.3 cm^3 to fit the values currently employed in AGM VRLA batteries. Since, the purpose of the cells used in the present study is to accelerate the ageing of the positive active-material, a ratio of positive active-material to negative active-material before formation of about 0.8 is employed. The cells (cf. Fig. 1) are designed with two negative electrodes and one positive electrode. The positive active-material is thus working more deeply than the negative active-material and its degradation is correspondingly rapid.

Two wedges provide constant pressure within the cell. Air tightness is obtained by means of a PTFE joint which is secured to the cell body by polypropylene screws. The gas pressure in the cell is regulated by a valve. Thus, the experimental results may be compared with those obtained with EV lead-acid batteries.

2.2. Electrical tests

Electrical tests were performed with Bitrode equipment which was controlled by computer.

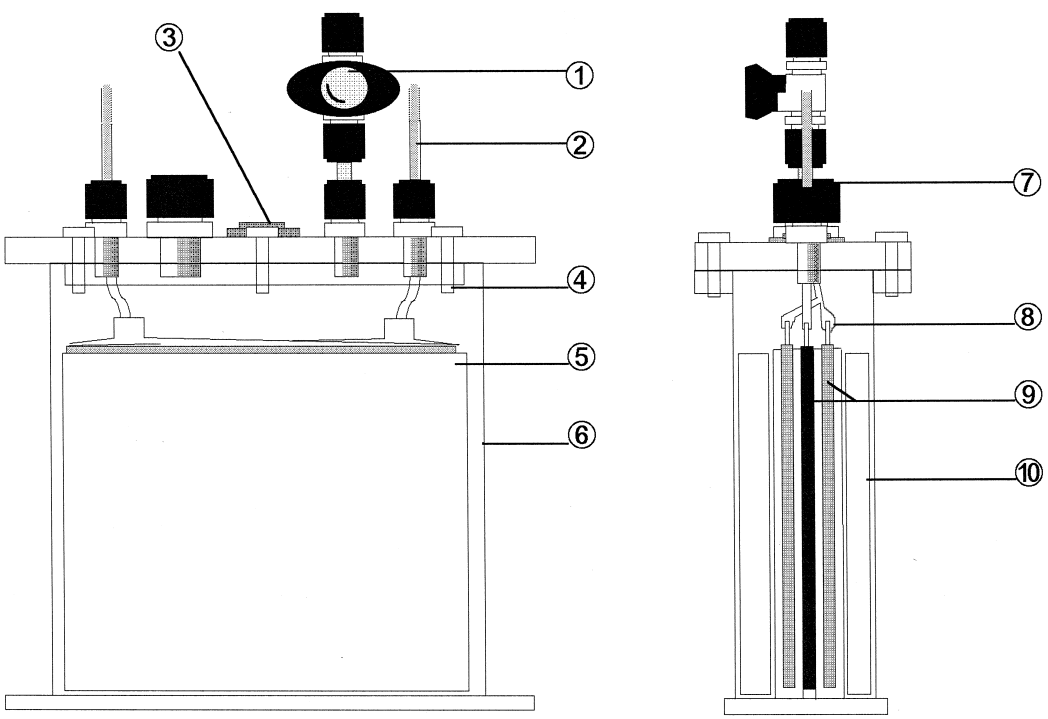

① Air tightness gate (teflon PFA) allowing a flooded use of the cell
② Positive connection lead
③ Valve for pressure regulation
④ Screw
⑤ Glass fibre separator around the - electrodes
⑥ Polycarbonate wall
⑦ Chromatography septum (teflon PFA)
⑧ Weld between electrodes and connections
⑨ Positive electrode between two negative electrodes
⑩ Polycarbonate fixing

Fig. 1. Valve-regulated cell used for all cycle-life tests.

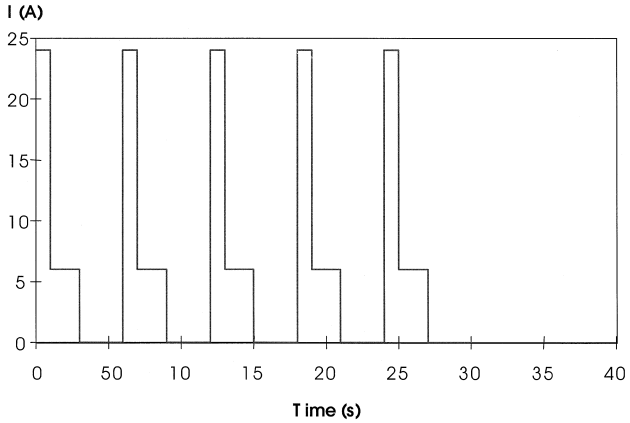

Fig. 2. Dynamic discharge, microcycles of TC69WG3 procedure.

Formation of the positive active-mass was conducted at 55°C in sulfuric acid (relative density: 1.20 g cm^{-3}) + Na_2SO_4 by applying a current of 2.5 A for 47 h. A low current (1.53 A) was always used during the first discharge in order to characterize the initial performance of the cells. The initial performance was always about 100 to 110 A h per kilogram of positive active-material. After this step, a standard profile, TC69WG3, was applied to simulate EV use (Fig. 2). This profile consists of a series of microcycles that contain two pulses of discharge (10 s at 24 A, 20 s at 6 A) followed by a 30-s rest. The discharge stops when the voltage reaches 1.6 V $cell^{-1}$.

The charge profile is comprised of three steps: (i) constant current (1.53 A) until the potential of the cell reaches 2.6 V; (ii) constant voltage until 103% of the previous discharge capacity is reached; (iii) constant current (0.150 A) for 2 h (Fig. 3).

The cycling of each cell was stopped at a defined moment in the cycle-life in order to observe the kinetics of the evolution of the positive active-material. The total capacity delivered by the active mass during its cycle life is given in ampere hour.

3. Quantitative analyses

During cycling, the composition of the active material was studied by using chemical measurements (Mettler Toledo material), X-ray diffraction analysis (CPS 120 INEL), and scanning electron microscopy (SEM) (JEOL JSM 35CF).

Chemical analysis shows that the positive active-material before cycling is composed of PbO_2 (between 95 and 100 wt.%) and $PbSO_4$ (very small quantities). Cycled materials contain the same compounds at the same proportions.

A quantitative approach can be achieved by means of X-ray diffraction phase analysis. This method enables crystalline varieties to be distinguished. In fact, the precision is about 4 wt.% when using the PEAKS software developed by CSIRO (Australia) [10–14]. The X-ray diffraction spectra show that the crystalline variety α-PbO_2 disappears during cycling (Fig. 4). In fact, this phenomenon depends of the electrolyte acidity. The α-PbO_2 variety is unstable at low pH, so the formation of β-PbO_2 is easier during charging. This is why only β-PbO_2 is found in the positive active-material at the end of cycling.

3.1. Study of micro-textural evolution

The micro-textural evolution of the active material consists of different changes at around the nm size. Specific surface area measurements and the SEM observations have been used in order to quantify this kind of evolution.

3.1.1. BET specific surface area measurements

Two types of electrode were investigated, namely, those cycled with low-current discharges and those cycled with TC69WG3 dynamic discharges. For electrodes cycled at the $C/10$ discharge rate, analyses of the charged state showed that the specific surface area, S, decreases during cycling from 3.5 to 2.6 m^2 g^{-1} (Fig. 5). The electrodes cycled under the TC69WG3 discharge profile display the same ageing to those cycled at the $C/10$ rate (Fig. 6). The

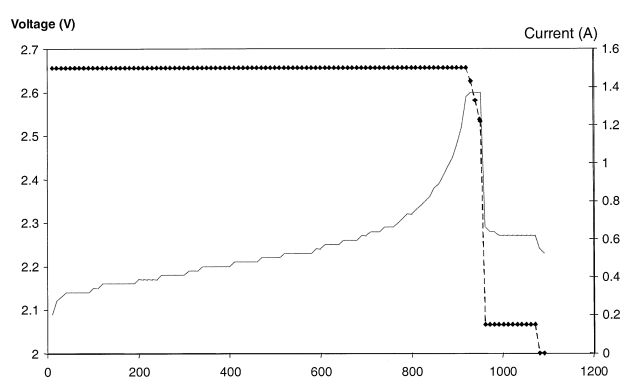

Fig. 3. Charge profile for 2-V cells. Voltage (————); current (– ♦ –).

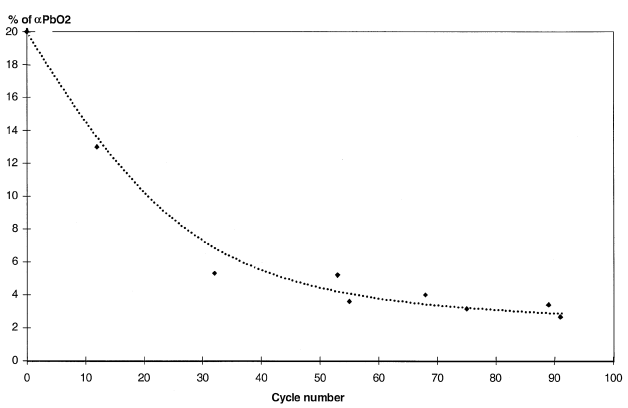

Fig. 4. Change in β-PbO_2 content during cycling.

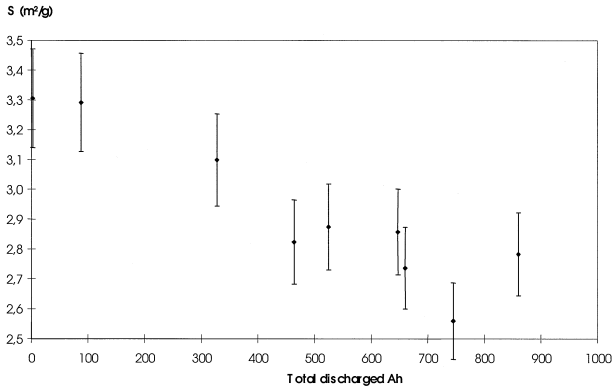

Fig. 5. Specific surface area, S of positive active-material cycled at the $C/10$ discharge rate.

main difference between these active materials is the kinetics of the decrease in specific surface area. In fact, the decrease is faster in the case of dynamic discharges: S falls from 3.5 to 1.7 $m^2\ g^{-1}$. It is observed in Fig. 6 that the active material cycled under EV duty has a BET surface area evolution close to that of the experimental cells.

3.1.2. SEM analyses

Electron micrographs show that the size of the β-PbO_2 grains increases during cycling. The general aspect of the active material changes and becomes spongy (Figs. 7 and 8).

As seen above, whatever the discharge profile, the specific surface area decreases during cycling. The study shows that active material cycled with the dynamic discharge profile reaches lower values of S than electrodes discharged with a low current. Therefore, these facts indicate that the S values are related to the active-mass utilization and the discharge profile.

The SEM observations confirm the evolution of S: there is a continuous growth of the β-PbO_2 grains during cycling. In fact, while the grain size is increasing, both the porosity and the BET surface area decrease. These analyses reveal the micro-textural evolution (μm scale) of the positive active-material during cycling and the link between the ageing kinetics and the discharge profile.

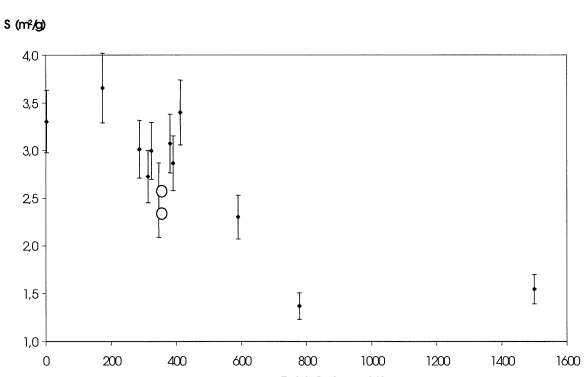

Fig. 6. Specific surface area, S, for positive active-material cycled: (•) under a TC69WG3 discharge profile; (◦) in an electric vehicle.

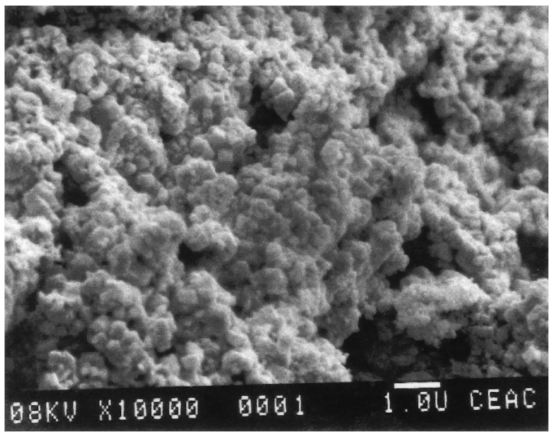

Fig. 7. Positive active-material before cycling.

3.2. Study of nano-textural evolution

This study was realized by means of two methods: (i) X-ray diffraction; (ii) electron microscopy using backscattered electrons, which gives a chemical contrast between the different components (PbO_2, $PbSO_4$, PbO, etc.).

3.2.1. X-ray diffraction

The β-PbO_2 crystallites represent the major portion of the positive active-material. The diffraction peaks are located by using the JCPDS file. The size of the β-PbO_2 crystallites, t, has been computed from the Laue–Scherrer relation [15], i.e.,

$$t = \frac{\lambda}{\Delta\theta \times \cos\theta} \quad (1)$$

where λ is the wavelength; θ is the diffraction angle; $\Delta\theta$ is the full width at half maximum. The latter is defined by the relation:

$$\Delta\theta = \sqrt{\left(\Delta\theta_M^2 - \Delta\theta_I^2\right)} \quad (2)$$

where $\Delta\theta_M$ is the measured width of the incident ray; $\Delta\theta_I$ is the instrumental width.

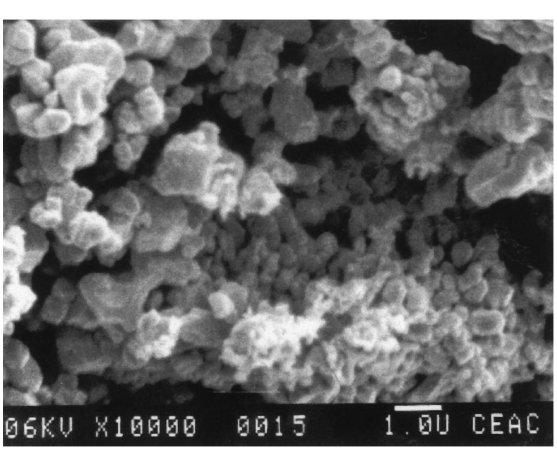

Fig. 8. Positive active-material after cycling (total discharged capacity: 500 A h).

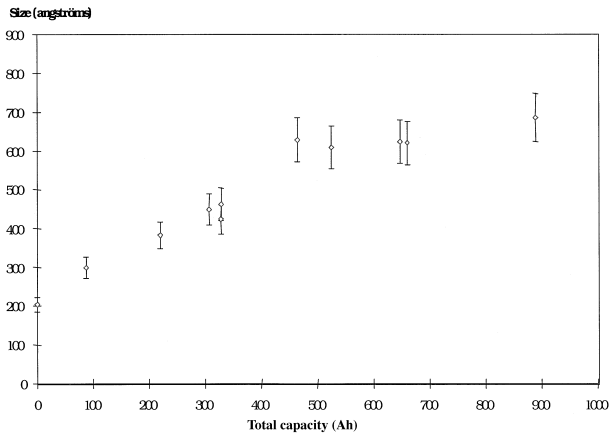

Fig. 9. Change in β-PbO_2 crystallite size (low current discharge).

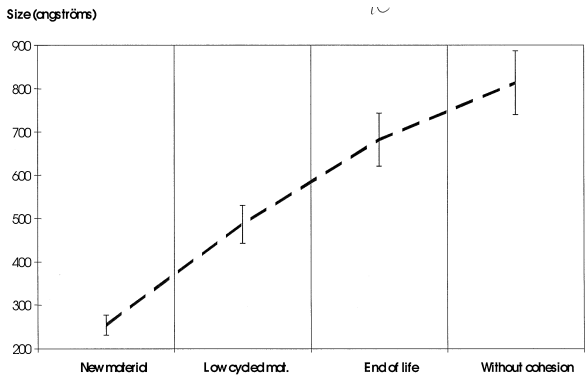

Fig. 11. Change in β-PbO_2 crystallite size during cycling.

At first, the evolution of active material was studied with low current discharge (1.53 A at 25°C). In this case, the electrochemical reactions are not limited by sulfuric acid diffusion. Each cell is deliberately stopped during its cycling in order to observe the positive electrode ageing (Fig. 9). There is a continuous growth of the β-PbO_2 crystallites throughout the life of these cells (from 20 to 75 nm).

With the dynamic discharge profile (TC69WG3), the same phenomenon (Fig. 10) is observed: the size of the crystallites increases from 20 to 75 nm. The growth kinetics are faster than those observed with electrodes cycled at low currents. These analyses point out the impact of the discharge profile on the ageing of the positive active-material.

Analysis was also undertaken of crystallites which have lost contact with the electrode during cycling. The results show that the crystallite size is greater for the active material without cohesion than for the β-PbO_2 connected to the bulk of the electrode (80–90 nm vs. 40–50 nm). It seems that the nano-textural ageing is linked to softening of the positive active-material. Beyond a size threshold, the β-PbO_2 crystallites appear to lose contact with each other; the electrode material conductivity declines and the electrochemical reactions are limited. The β-PbO_2 nano-textural evolution during cycling is shown in Fig. 11.

The X-ray diffraction analyses show that the growth of the β-PbO_2 crystallites depends on the stress imposed on the electrode material. The analyses also reveal the link between the positive material softening and the β-PbO_2 nano-textural evolution during cycling. In fact, there is a continuous crystallites size growth all along the cycle life until the final disconnection. The disconnection size threshold depends on other cell parameters such as porosity, specific surface area, initial active-material composition, etc.

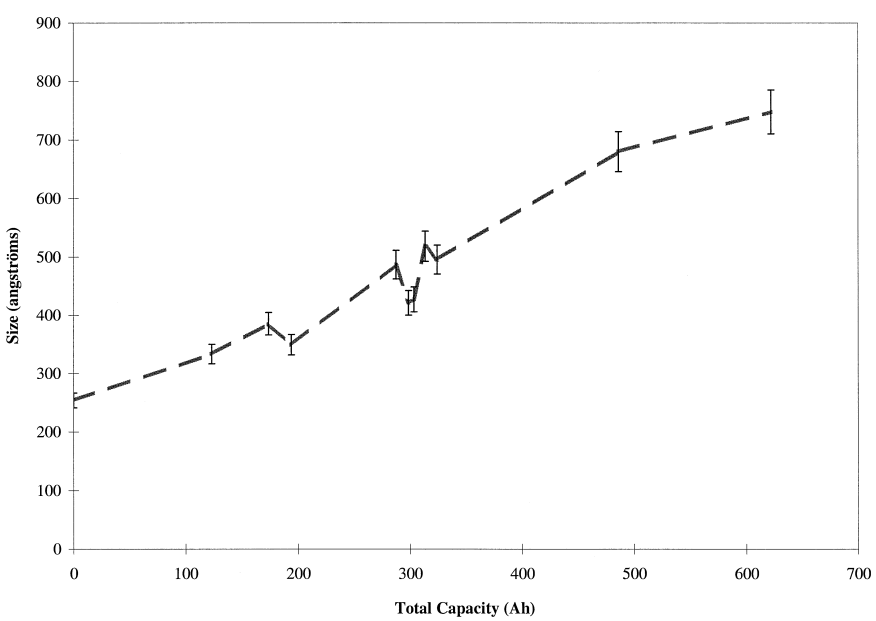

Fig. 10. Change in β-PbO_2 crystallite size (dynamic discharge profile).

3.2.2. SEM using back-scattered electrons

This method provides confirmation of the X-ray diffraction measurements. The chemical contrast reveals the β-PbO_2 crystallites in the bulk of the positive material. Comparison of electron micrographs confirms the growth in crystallite size during cycling (Figs. 12 and 13). The size of the β-PbO_2 crystallites increases from 30 to 90–100 nm.

3.3. Model for micro- and nano-textural evolution

The micro-textural and the nano-textural evolution of the positive active-material during cycling have been observed. The kinetics depend on the cycling conditions. The growth of the grains parallels the increase in crystallite size. The nano-textural evolution stops when the β-PbO_2 crystallites are too large; they lose contact with the positive plate and no longer take part in the electrochemical reactions.

These changes are in accordance with the Kugelhaufen Model developed by Bashtavelova and Winsel [16], Pohl and Rickert [17], and Morris et al. [18]. The active material can be considered to be an 'aggregate of spheres'. The specific resistance of the aggregate can be linked to the sphere dimensions by the following relation:

$$\bar{\omega} \cong \omega(R/h) \tag{1a}$$

where $\bar{\omega}$ is the specific resistance of the sphere aggregate, ω is the specific resistance of the bulk β-PbO_2; R is the radius of the sphere; h is the radius of the neck zone.

The conductivity of the positive material is determined by the value of the R/h ratio. It changes with the radius of the neck zones. On one hand, if these contact points are too small, the active material tends to become isolating. On the other hand, if the number of the neck zones is not sufficient, the conductivity decreases. Thus, the optimum functioning of the positive material depends on the balance between the number of neighbours around each sphere and the size of the neck zones.

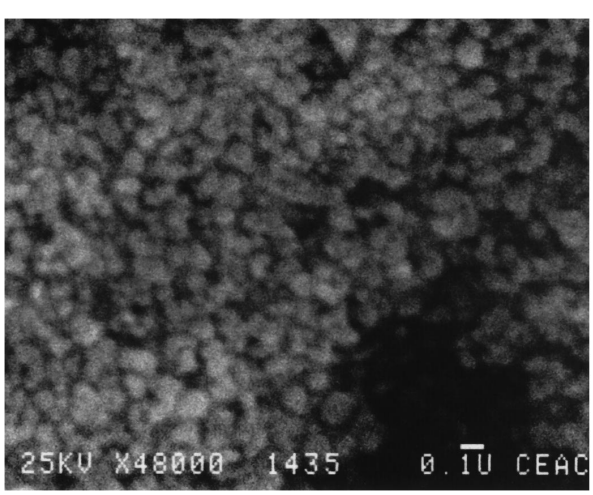

Fig. 12. Electron micrograph using back-scattered electrons to provide a chemical contrast. Active material before cycling.

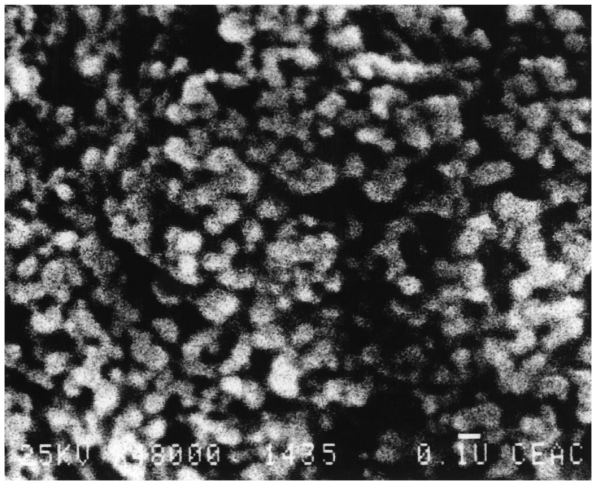

Fig. 13. Electron micrograph using back-scattered electrons to provide a chemical contrast. Active material after cycling with dynamic discharges.

Winsel et al. [14] have determined that the potential difference between the β-PbO_2 spheres and the neck zones influences the structure of the active material. The degree of disorganization of the spheres and at the neck zones is denoted by δ_R and δ_h, respectively. Pohl and Rickert [17] have shown that a relation exists between the potential, ϕ, and the degree of disorganization, δ. Winsel et al. [14] have extrapolated the following relation:

$$\log\frac{\delta_h}{\delta_R} = 8.04\frac{V_0\sigma_0}{FR}\left(1+\frac{R^2}{h^2}\right) \tag{4}$$

where R is the sphere radius (cm); h is the neck zone radius; V_0 is the β-PbO_2 molar volume; σ_0 is the β-PbO_2 surface tension in sulfuric acid; F is the Faraday constant. The limiting values of the disorganization degree are $3\times10^{-3} < \delta < 1.6\times10^{-2}$. The PbO_2 surface tension, σ_0, in dilute sulfuric acid (relative density = 1.30 g cm^{-3}) is estimated to be 10^{-4} J cm^{-2}. The PbO_2 molar volume value is $V_0 = 24.6$ cm^3 mol^{-1}.

For an active material before cycling, $R = 0.3\times10^{-5}$ cm. Thus, the first term of Eq. (4) becomes:

$$8.04\frac{V_0\sigma_0}{FR} = 0.0683. \tag{5}$$

Using the limiting values of δ given by Bullock [19] yields:

$$\log\frac{\delta_h}{\delta_R} \le \log\frac{\delta_{max}}{\delta_{min}} \tag{6}$$

$$\log\frac{\delta_h}{\delta_R} \le 0.727. \tag{7}$$

Eqs. (4)–(7) give:

$$0.727 \ge 0.0683\left(1+\frac{R^2}{h^2}\right) \tag{8}$$

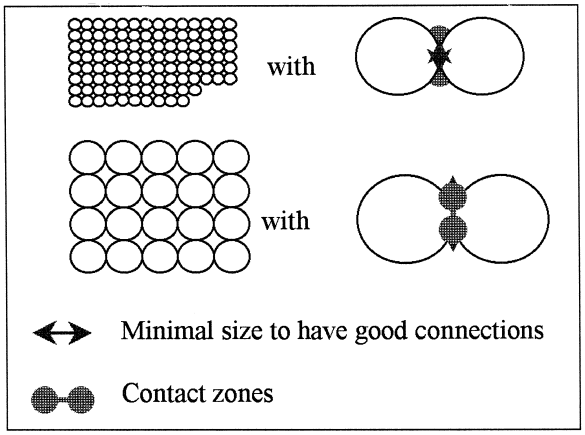

Fig. 14. Representation of positive active-material evolution before cycling (top) and after cycling (bottom) according to the Kugelhaufen Model.

and

$$\frac{R}{h} \leq 3.1 \qquad (9)$$

If $R = 3 \times 10^{-6}$ cm for positive active-material before cycling, as shown by the results of this study, the minimum value for h is 9.7 nm. Equally, if $R = 0.8 \times 10^{-5}$ cm for a positive active-material after cycling, the minimal value for h is 15.3 nm.

If a comparison is made of the minimum value of the neck zone radius computed for active material before and after cycling, the values are more than twice those for an active material analysed after cycling. The greater the size of the sphere, the greater the width of the neck zones to insure good conductivity of the β-PbO_2 network (cf. Fig. 14). This model can be used to explain these two evolution scales (micro- and nano-textural) from an electrical and a mechanical point of view.

The above study shows that there are two textural evolutions during cycling: micro- and nano-textural. It seems that the crystallite size is the main determinant of positive active-material ageing. The disconnection of crystallites from the electrode is closely linked to the continuous nano-textural growth. The impact of the discharge profile on the β-PbO_2 ageing kinetics is also demonstrated. A dynamic discharge profile accelerates the damage to the β-PbO_2 texture, with a decrease of crystallite contacts and, then, a reduction in conductivity.

Technical solutions were used in attempts to extend the life of lead-acid cells. Thus, phosphoric acid was added to the electrolyte.

4. Phosphoric acid addition

This additive has been used in lead-acid batteries from the beginning of the century in order to reduce electrode sulfation in deep discharge. It has also been used in order to decrease positive material damage in flooded lead-acid batteries. For these reasons, it was decided to add this compound to the new AGM technology batteries developed here.

The experimental cells were the same as for the first part of this study; their characteristics permit acceleration of active-material ageing. The cycling discharge and charge profiles were also identical. Phosphoric acid (2.2 wt.%) was added to the electrolyte before cycling.

The cycle-life is superior for cells with phosphoric acid, see Fig. 15. The performance was initially lower than that for cells without phosphoric acid. But after a few cycles, the specific capacity tends to be more stable in the presence of the electrolyte additive. Thus, phosphoric acid addition could be helpful to extend the cycle-life of AGM cells.

The positive active-material cycled in a cell containing phosphoric acid has been analysed and compared with that from reference cells. Electron microscopy using secondary electrons reveals that the β-PbO_2 grains are smaller in the cell containing phosphoric acid. The active material is also more compact when H_3PO_4 is added. These features have been already explored in previous studies [20]. X-ray diffraction analyses show that phosphoric acid influences the β-PbO_2 nano-textural characteristics (Fig. 16). The crystallite size is smaller in cycled cells containing H_3PO_4 than in cycled reference cells. Furthermore, the crystallite size is very stable during cycling: the average size is about 35 nm which is very close to the value before cycling (30 nm). The low nano-textural evolution could explain the stability in performance during cycling. Addition of H_3PO_4 also appears to increase the cycle-life of AGM lead-acid batteries by favouring small micro- and nano-textures. The size of the β-PbO_2 crystallites stays under 40 nm. The above observations are in accordance with our previous conclusions and the Kugelhaufen Model. The small crystallite size tends to improve the stability of the positive material (small contact radius between spheres); in fact, there is almost no softening in cells containing phosphoric acid, even with dynamic cycling.

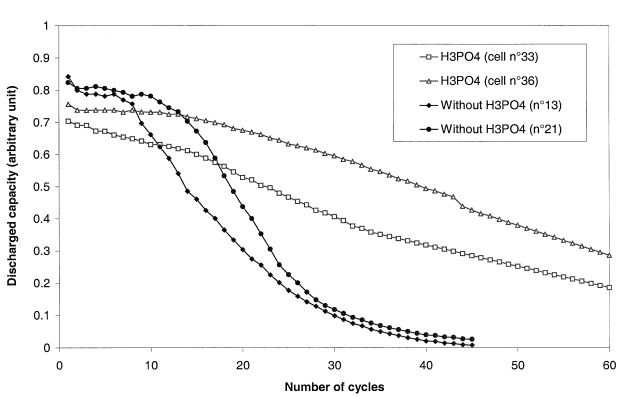

Fig. 15. Cells performance: (·, ♦) with phosphoric acid; (◦, ◇) without phosphoric acid. The three first cycles were conducted with a $C/10$ discharge profile; a TC69WG3 discharge profile was then used.

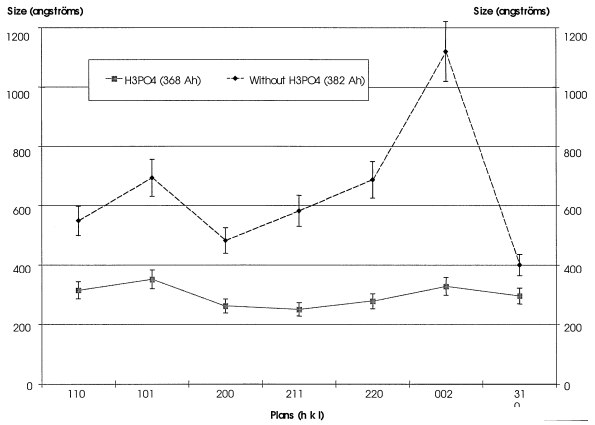

Fig. 16. Influence of H_3PO_4 on the β-PbO_2 nano-texture.

The main disadvantage with using phosphoric acid is a decrease in the initial performance. The cells lose almost 10% of their specific capacity at the beginning of their cycle-life. This phenomenon is linked to the electrochemical behaviour of H_3PO_4: the additive limits the kinetics of the discharge reaction [21,22]. On the other hand, the loss in specific capacity is compensated by an improved cycle-life.

5. Electrical treatment

It has been found that the discharge profile determines the ageing kinetics of the positive active-material. In all the cases, the β-PbO_2 texture grows; finally, the crystallites lose contact with each other and the active material becomes disconnected. It is possible that electrochemical treatment can restore the performance of the battery. This method has been investigated with gel lead-acid batteries, but not with AGM batteries [13,14]. Thus, the following experimental programme was undertaken.

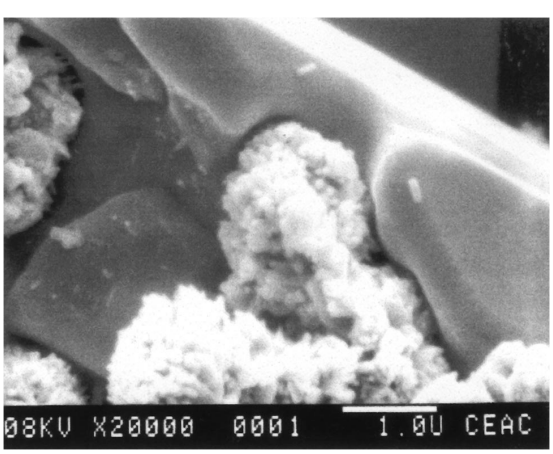

Fig. 17. Electron micrograph using secondary electrons. The observed β-PbO_2 crystals are on $PbSO_4$.

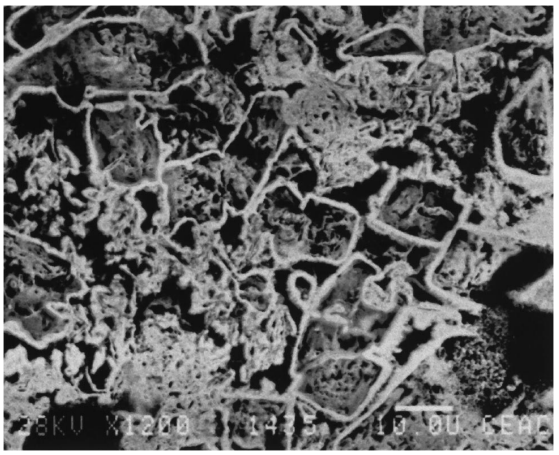

Fig. 18. Electron micrograph using back-scattered electrons. β-PbO_2 crystals (white) are present on the edges of $PbSO_4$ crystals (grey).

Experiments were performed on the same cells as those used for the active-material ageing study. These were subjected to the TC69WG3 discharge profile. All the cycling characteristics are similar. When the specific capacities of the cells reached critical values corresponding to one-third of the dynamic discharge nominal capacity, an electrical treatment was applied. The treatment comprised deep discharge with a very low current (0.75 A). The discharge was terminated when the cell voltage reached 1.4 V. The following charge had a classical profile with three steps (see Fig. 3) and returned 110% of the discharged capacity.

Although there was an improvement in cell performance after electrical treatment, the effect did not last long and the battery capacity declined again after a few cycles. After several treatments, the efficiency of this technique became limited, i.e., the cell sensitivity decreased with the number of cycles. It seems that the efficacy of the electrical treatment is closely linked to the ageing of the active

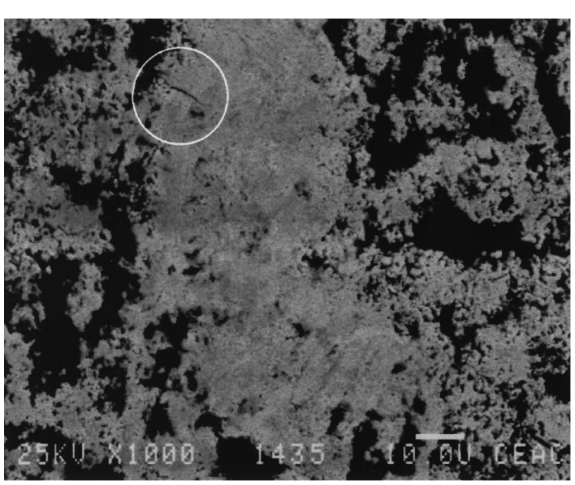

Fig. 19. Electron micrograph using back-scattered electrons. β-PbO_2 crystals are agglomerated in the positive active-material.

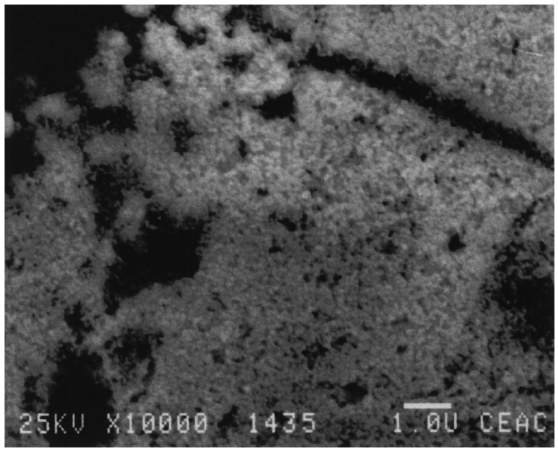

Fig. 20. Electron micrograph using back-scattered electrons. An agglomerate of β-PbO_2 crystallites is clearly observable.

material. Thus, each cell was analyzed in order to understand physicochemical changes in the active material during deep-discharge treatment.

5.1. Micro-textural analysis

Scanning electron micrographs reveal β-PbO_2 crystallization mechanisms which take place on the $PbSO_4$ surface during recharge. Scanning with a secondary electron signal provides a topographic contrast and the back-scattered electron signal provides a chemical contrast. Figs. 17 and 18 show the β-PbO_2 crystallization and crystal growth, respectively. The nucleation begins on the surface of the $PbSO_4$ crystals where the electronic and ionic conductivity permits this phenomenon (crystals edges and lattice defects) [23]. The β-PbO_2 nuclei develop both on and in the $PbSO_4$ crystals; the lead sulfate is consumed during recharge. It is noted that large $PbSO_4$ crystals yield denser β-PbO_2 agglomerates than small $PbSO_4$ crystals. The effect of deep-discharge may be linked to the formation of a compact crystal network during the oxidation of large $PbSO_4$ crystals.

The above characteristics could improve the electronic and ionic transfer that is required during charge–discharge reactions. Also, the expansion of the positive active-mass would be prevented locally. This hypothesis was tested by means of SEM (Figs. 19 and 20). The micrographs show that a treated active mass consists essentially of β-PbO_2. Recently recharged, compact aggregates of crystallites are observed at locations where the crystallites are very close to each other.

5.2. Nano-textural analyses

X-ray diffraction analysis allows observation of the evolution of crystallite size during cycling with or without electrical treatment (Fig. 21). The size comparison shows that the deep discharges act on the active-material nano-texture: the crystallite growth is smaller in the case of active material with electrical treatment. This difference is higher when the positive material is older. It should be pointed out, however, that electrical treatment cannot restore the initial state of the active material, i.e., its effect is partial.

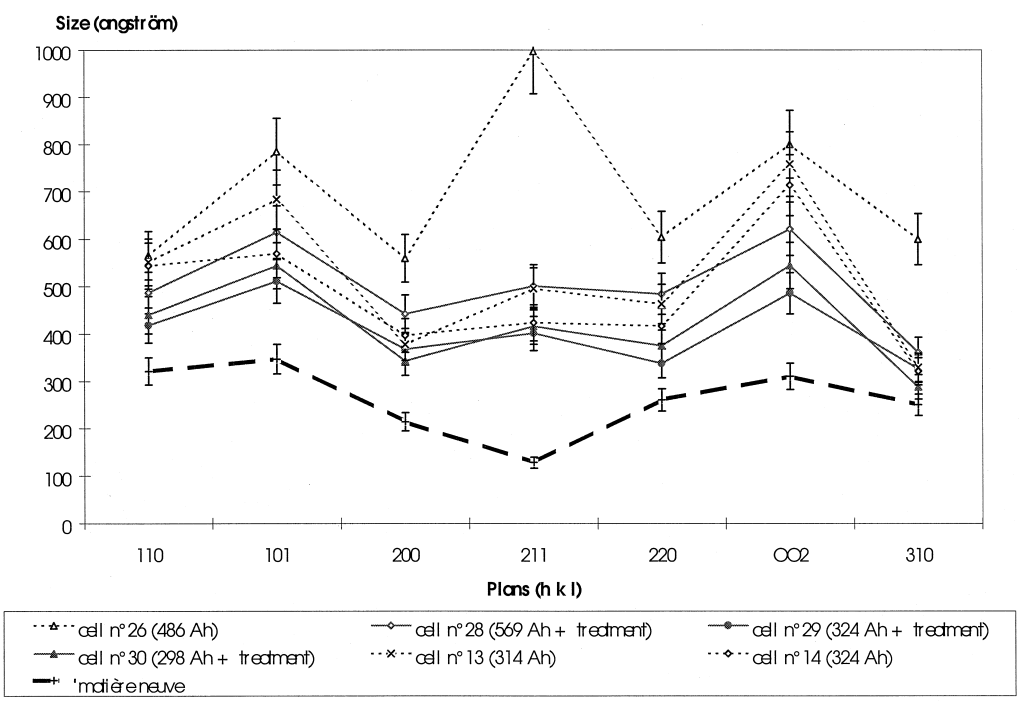

Fig. 21. Crystallite size, with or without electrical treatment, during cycling.

5.3. Summary

Studies of active material subjected to regular deep-discharge treatment reveals the different effects caused by this method. Textural changes are observed. Deep discharge favours the formation of large $PbSO_4$ crystals. These crystals are oxidized to form compact β-PbO_2 agglomerates during recharge. As a consequence, the micro-texture of the positive material is improved. Concomitantly, electrical treatment maintains a small β-PbO_2 crystallite size in the active mass. (Note, crystallite size is the main ageing parameter during cycling). Nevertheless, the initial size of the crystallites is never regained with this electrical treatment. Unfortunately, the improvement in cell performance is not sustained. The micro-textural changes are clear but the nano-textural effect is rather small. The state of the active material during cycling depends essentially on the size of the β-PbO_2 crystallites. Deep discharge provides only a local restoration of battery performance.

6. Conclusions

Experimental AGM-type lead-acid cells have been developed in order to observe ageing of the positive active-material during dynamic cycling. These cells allow acceleration of positive material ageing.

Analysis of the positive active-material has revealed a decrease in the specific surface area and crystal growth during cycling: a micro-textural evolution is observed. X-ray diffraction experiments provide information on nano-textural evolution during cycling, the kinetics of which depend on the discharge profile: a discharge profile with high current discharge pulses accelerates softening of the active mass. These analyses were confirmed by SEM with back-scattered electrons: the β-PbO_2 crystallites grow from 30 to almost 100 nm. It seems that active-material softening is determined by a critical size value (around 90–100 nm). These results show that growth of crystallite size is the key parameter of positive mass ageing. Small crystallites insure a good crystalline network and optimum electronic and ionic conductivity.

Two methods are promising for restoration of battery performance, namely, a chemical method and an electrical treatment. A chemical approach is to add phosphoric acid to the electrolyte. This additive is incorporated in the active material during recharge and preserves crystallite size during cycling. The battery capacity is stabilized and the cycle-life is extended. The only disadvantage of this approach is a loss 10% of initial battery capacity.

Electrical treatment uses deep discharges and partially restores the micro- and nano-texture of the β-PbO_2. The cell performance is restored, but is not sustained: the specific capacity declines after a few cycles.

A strategy to extend battery cycle-life could be a combination of the above two methods: H_3PO_4 addition would stabilize the β-PbO_2 nano-texture at close to its initial value, while electrical treatment could be useful in restoring the capacity during cycling. This approach could ensure good reliability of lead-acid batteries in electric-vehicle use.

Acknowledgements

The authors are especially grateful to Hagen Batteries, EDF, and Renault V.E. for their contribution to this study. Thanks are also due to ADEME for its financial contribution (contract No. 95.91.014).

References

[1] J.R. Pierson, Electrochem. Technol. 5 (1967) 12.
[2] K. Harris, R.J. Hill, D.A.J. Rand, J. Power Sources 8 (1982) 175.
[3] V.H. Dodson, J. Electrochem. Soc. 108 (1961) 401.
[4] V.H. Dodson, J. Electrochem. Soc. 108 (1961) 406.
[5] B. Culpin, J. Power Sources 25 (1989) 305.
[6] P. Boher, Thèse, Université Pierre et Marie Curie, Paris, 1984.
[7] R.J. Hill, I.C. Madsen, J. Electrochem. Soc. 131 (1984) 1486.
[8] D. Pavlov, J. Power Sources 11 (1986) 165.
[9] D. Pavlov, E. Bashtavelova, J. Electrochem. Soc. 131 (1984) 1468.
[10] R.J. Hill, Mat. Res. Bull. 17 (1982) 769.
[11] R.J. Hill, J. Power Sources 11 (1984) 19.
[12] R.J. Hill, I.C. Madsen, J. Electrochem. Soc. 131 (1984) 1486.
[13] J.P. Eberhart, Analyse structurale et chimique des matériaux, Dunod, Bordas, Paris, 1989.
[14] A. Winsel, E. Voss, U. Hullmeine, J. Power Sources 30 (1993) 209.
[15] A. Winsel, E. Bashtavelova, J. Power Sources 46 (1993) 211.
[16] E. Bashtavelova, A. Winsel, J. Power Sources 46 (1993) 219.
[17] J.P. Pohl, H. Rickert, Electrodes of Conductive Metallic Oxides, Elsevier, Amsterdam, 1980, p. 184.
[18] G.A. Morris, P.J. Mitchell, N.A. Hampson, J.J. Dyson, J. Power Sources 30 (1990) 61.
[19] K.R. Bullock, J. Electrochem. Soc. 124 (1977) 1478.
[20] K.R. Bullock, J. Electrochem. Soc. 126 (1979) 1848.
[21] S. Venugopalan, J. Power Sources 46 (1993) 1.
[22] L.T. Lam, H. Ozgun, O.V. Lim, J.A. Hamilton, L.H. Vu, D.G. Vella, D.A.J. Rand, J. Power Sources 53 (1995) 215.
[23] A. Chraa, Thèse de doctorat de l'Université Pierre et Marie Curie, Paris, 1993.